[9] M. F. Millea, M. McColl, and C. A. Mead, "Schottky barriers on GaAs," *Phys. Rev.*, vol. 177, pp. 1164–1172, Jan. 1969.
[10] A. A. M. Saleh, "Theory of resistive mixers," Ph.D. dissertation, M.I.T., Cambridge, MA, 1970.
[11] S. M. Sze, *Physics of Semiconductor Devices*, New York: Wiley, 1969.
[12] M. McColl, R. J. Pedersen, M. F. Bottjer, M. F. Millea, A. H. Silver, and F. L. Vernon, Jr., "The super-Schottky diode microwave mixer," *Appl. Phys. Lett*, vol. 28, pp. 159–162, Feb. 1, 1976.
[13] S. Weinreb and A. R. Kerr, "Cryogenic cooling of mixers for millimeter and centimeter wavelengths," *IEEE J. Solid-State Circuits (Special Issue on Microwave Integrated Circuits)*, vol. SC-8, pp. 58–63, Feb. 1973.
[14] A. R. Kerr, "Low-noise temperature and cryogenic mixers for 80–120 GHz," *IEEE Trans. Microwave Theory Tech.*, vol. MTT-23, pp. 781–787, Oct. 1975.
[15] H. M. Day, A. C. Macpherson, and E. F. Bradshaw, "Multiple contact Schottky barrier microwave diode," *Proc. IEEE* (Corresp.), vol. 54, pp. 1955–1956, Dec. 1966.
[16] M. McColl and M. F. Millea, "Advantages of Mott barrier mixer diodes," *Proc. IEEE* (Corresp.), vol. 61, pp. 499–500, Apr. 1973.
[17] T. J. Viola, Jr., and R. J. Mattauch, "Unified theory of high-frequency noise in Schottky barriers," *J. Appl. Phys.*, vol. 44, pp. 2805–2808, June 1973.
[18] D. T. Hodges and M. McColl, "Extension of the Schottky barrier detector to 70 μm (4.3 THz) using submicron-dimensional contacts," *Appl. Phys. Lett.*, vol. 30, pp. 5–7, Jan. 1, 1977.
[19] M. McColl, D. T. Hodges, and W. A. Garber, "Submillimeter-wave detection with submicron size Schottky barrier diodes," presented at the 2nd Int. Conf. and Winter School on Submillimeter Waves and Their Applications, San Juan, Puerto Rico, Dec. 6–11, 1976.

Mode Classification of a Triangular Ferrite Post for *Y*-Circulator Operation

YOSHIHIKO AKAIWA

***Abstract*—Resonance modes of a triangular ferrite post are classified into those which correspond to each eigen-excitation in order to select operation modes of the *Y* circulator. Resonance frequency splits for two rotational phase eigen-excitations are also discussed.**

Introduction

Resonance modes of full height as well as partial-height ferrite junction circulators were studied recently [1]–[3]. Among the various resonance modes, special modes, which correspond to the rotational phase eigen-excitations, principally support the circulator operation. Operation modes are those which have no zero- or threefold symmetry around the ferrite post axis for the *Y* circulator. For a cylindrical ferrite post, operation modes can be easily selected, owing to the field distribution simplicity.

The purpose of this short paper is to classify the resonance modes of a triangular ferrite post into those which correspond to each eigen-excitation in order to select operation modes. The resonance frequencies split, which is one of the fundamental parameters for circulator operation, is also discussed under the assumption of a small anisotropy.

Resonance Mode Classification for Each Eigen-Excitation

In a case of a small anisotropy, the fields in the magnetized ferrite post may be given approximately from those of the demagnetized ferrite post, i.e., dielectric post, using a perturbation theory. Circulation occurs with the pairs of resonance modes which are degenerate when the ferrite is demagnetized. Therefore, we consider the fields in the demagnetized ferrite post. Assuming TM modes and the completely open-circuited condition at the side wall of the ferrite post, the fields are given as follows:

$$E_z = \frac{\chi^2}{j\omega\varepsilon} T(x,y) e^{j\beta z} \tag{1}$$

$$T(x,y) = \cos\left[\frac{2\pi}{3b} l\left(\frac{x}{2} + b\right)\right] \cos\left(\frac{\sqrt{3}\pi(m-n)}{9b} y\right) + \cos\left[\frac{2\pi}{3b} m\left(\frac{x}{2} + b\right)\right] \cos\left(\frac{\sqrt{3}\pi(n-l)}{9b} y\right) + \cos\left[\frac{2\pi}{3b} n\left(\frac{x}{2} + b\right)\right] \cos\left(\frac{\sqrt{3}\pi(l-m)}{9b} y\right) \tag{2}$$

$$H_x = -j \frac{\omega\varepsilon}{\omega^2\varepsilon\mu - \beta^2} \frac{\partial E_z}{\partial y} \tag{3}$$

$$H_y = j \frac{\omega\varepsilon}{\omega^2\varepsilon\mu - \beta^2} \frac{\partial E_z}{\partial x} \tag{4}$$

$$H_z = 0 \tag{5}$$

$$E_x = -j \frac{\beta}{\omega\varepsilon} H_y \tag{6}$$

$$E_y = j \frac{\beta}{\omega\varepsilon} H_x \tag{7}$$

where b is the radius of the inscribed circle of the triangle, l, m, and n are integers which never take zero simultaneously and are related by the following equations:

$$l + m + n = 0 \tag{8}$$

and

$$\chi^2 = \left(\frac{4\pi}{3a}\right)^2 (m^2 + mn + n^2) \tag{9}$$

where a is the side length of the triangle, i.e.,

$$a = 2\sqrt{3}b.$$

These fields are represented by a standing wave in the x–y plane, since they are obtained from those of the triangular metal waveguide [4] by the duality concept. The fields corresponding to the eigen-excitations are traveling or rotating waves in the x–y plane, which take the following phase relation at the ports:

$$\phi_1 = \frac{1}{3}\begin{pmatrix}1\\1\\1\end{pmatrix} \qquad \phi_2 = \frac{1}{3}\begin{pmatrix}1\\e^{j(2/3)\pi}\\e^{-j(2/3)\pi}\end{pmatrix} \qquad \phi_3 = \frac{1}{3}\begin{pmatrix}1\\e^{-j(2/3)\pi}\\e^{j(2/3)\pi}\end{pmatrix} \tag{10}$$

where ϕ_1, ϕ_2, and ϕ_3 are the in-phase, clockwise, and counterclockwise rotational phase eigen-excitations, respectively. To classify the resonance modes, it is necessary to obtain fields which correspond to each eigen-excitation.

The fields given by (1)–(7) can be considered to be excited through one of the ports. It is assumed that the port is port 1, for convenience sake (see Fig. 1). The fields excited through other ports are given by the coordinate transformation

$$x \to -\frac{1}{2}x \mp \frac{\sqrt{3}}{2}y \tag{11}$$

$$y \to \pm\frac{\sqrt{3}}{2}x - \frac{1}{2}y \tag{12}$$

where the upper and lower signs denote the cases where excitation is through port 2 and port 3, respectively. Therefore, field

Manuscript received February 27, 1976; revised July 21, 1976.
The author is with the Central Research Laboratories, Nippon Electric Company Ltd., Kawasaki, Japan.

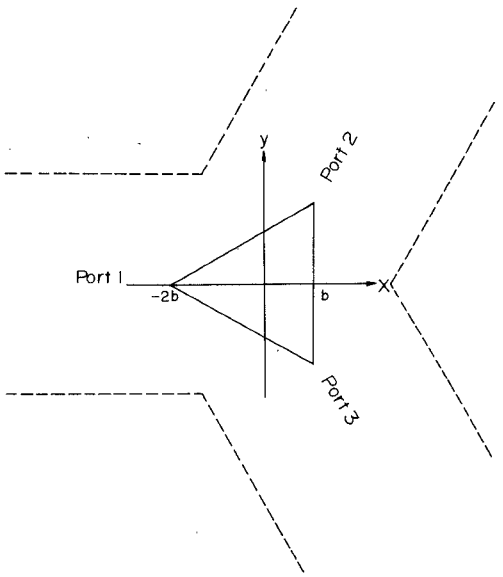

Fig. 1. Coordinates for triangular ferrite post used in a Y circulator.

distribution in the x–y plane can be given by

$$T_2(x,y) = T_1\left(-\frac{1}{2}x - \frac{\sqrt{3}}{2}y, \frac{\sqrt{3}}{2}x - \frac{1}{2}y\right) \tag{13}$$

$$T_3(x,y) = T_1\left(-\frac{1}{2}x + \frac{\sqrt{3}}{2}y, -\frac{\sqrt{3}}{2}x - \frac{1}{2}y\right) \tag{14}$$

where T_1, T_2, and T_3 denote the field distribution given by (2), corresponding to excitations through ports 1, 2, and 3, respectively.

Thus the fields for eigen-excitations can be obtained by the superimposition of the fields, taking into account the phase relations of (10).

For the in-phase eigen-excitation,

$$\begin{aligned}\Phi_1 &= \frac{1}{3}\{T_1(x,y) + T_2(x,y) + T_3(x,y)\}\\ &= \frac{1}{3}\left\{\cos\left(\frac{\pi l}{3b}x + \frac{2\pi}{3}l\right) + \cos\left(\frac{\pi l}{3b}x + \frac{2\pi}{3}m\right)\right.\\ &\quad\left. + \cos\left(\frac{\pi l}{3b}x + \frac{2\pi}{3}n\right)\right\}\cos\left(\frac{m-n}{3\sqrt{3b}}\pi y\right)\\ &\quad + \frac{1}{3}\left\{\cos\left(\frac{\pi m}{3b}x + \frac{2\pi}{3}m\right) + \cos\left(\frac{\pi m}{3b}x + \frac{2\pi}{3}l\right)\right.\\ &\quad\left. + \cos\left(\frac{\pi m}{3b}x + \frac{2\pi}{3}n\right)\right\}\cos\left(\frac{n-l}{3\sqrt{3b}}\pi y\right)\\ &\quad + \frac{1}{3}\left\{\cos\left(\frac{\pi n}{3b}x + \frac{2\pi}{3}n\right) + \cos\left(\frac{\pi n}{3b}x + \frac{2\pi}{3}l\right)\right.\\ &\quad\left. + \cos\left(\frac{\pi n}{3b}x + \frac{2\pi}{3}m\right)\right\}\cos\left(\frac{l-m}{3\sqrt{3b}}\pi y\right).\end{aligned} \tag{15}$$

The combinations of l, m, and n, which make (15) null are given as follows:

$$\begin{aligned} l &= 2p - q \pm 1\\ m &= 2q - p \mp 1\\ n &= -p - q\end{aligned} \tag{16}$$

where doubled signs are taken in the same order. The modes given by (16) have no symmetry of ϕ_1 in (10).

For the rotational phase eigen-excitations,

$$\begin{aligned}\Phi_{2,3} &= \tfrac{1}{3}\{T_1(x,y) + e^{\mp j(2/3)\pi}T_2(x,y) + e^{\pm j(2/3)\pi}T_3(x,y)\}\\ &= \frac{1}{3}\left[\left\{\cos\left(\frac{\pi l}{3b}x + \frac{2\pi}{3}l\right) - \frac{1}{2}\cos\left(\frac{\pi l}{3b}x + \frac{2\pi}{3}m\right)\right.\right.\\ &\quad\left.\left. - \frac{1}{2}\cos\left(\frac{\pi l}{3b}x + \frac{2\pi}{3}n\right)\right\}\cos\left(\frac{n-m}{3\sqrt{3b}}\pi y\right)\right.\\ &\quad + \left\{\cos\left(\frac{\pi m}{3b}x + \frac{2\pi}{3}m\right) - \frac{1}{2}\cos\left(\frac{\pi m}{3b}x + \frac{2\pi}{3}l\right)\right.\\ &\quad\left. - \frac{1}{2}\cos\left(\frac{\pi m}{3b}x + \frac{2\pi}{3}n\right)\right\}\cos\left(\frac{l-n}{3\sqrt{3b}}\pi y\right)\\ &\quad + \left\{\cos\left(\frac{\pi n}{3b}x + \frac{2\pi}{3}n\right) - \frac{1}{2}\cos\left(\frac{\pi n}{3b}x + \frac{2\pi}{3}l\right)\right.\\ &\quad\left. - \frac{1}{2}\cos\left(\frac{\pi n}{3b}x + \frac{2\pi}{3}m\right)\right\}\cos\left(\frac{m-l}{3\sqrt{3b}}\pi y\right)\\ &\quad \mp j\frac{\sqrt{3}}{2}\left\{\sin\left(\frac{\pi n}{3b}x + \frac{2\pi}{3}l\right)\right.\\ &\quad\left. - \sin\left(\frac{\pi n}{3b}x + \frac{2\pi}{3}m\right)\right\}\sin\left(\frac{l-m}{3\sqrt{3b}}\pi y\right)\\ &\quad \mp j\frac{\sqrt{3}}{2}\left\{\sin\left(\frac{\pi l}{3b}x + \frac{2\pi}{3}m\right)\right.\\ &\quad\left. - \sin\left(\frac{\pi l}{3b}x + \frac{2\pi}{3}n\right)\right\}\sin\left(\frac{m-n}{3\sqrt{3b}}\pi y\right)\\ &\quad \mp j\frac{\sqrt{3}}{2}\left\{\sin\left(\frac{\pi m}{3b}x + \frac{2\pi}{3}n\right)\right.\\ &\quad\left.\left. - \sin\left(\frac{\pi m}{3b}x + \frac{2\pi}{3}l\right)\right\}\sin\left(\frac{n-l}{3\sqrt{3b}}\pi y\right)\right]\end{aligned} \tag{17}$$

where the upper and lower signs denote the cases of clockwise and counterclockwise rotational eigen-excitation, respectively. The combinations of l, m, and n, which make (17) null, are given as follows:

$$\begin{aligned} l &= 2p - q\\ m &= 2q - p\\ n &= -p - q, \qquad p,q = 0,\pm1,\pm2,\cdots.\end{aligned} \tag{18}$$

The modes given by (18) have no symmetry of ϕ_2 and ϕ_3. These modes are not the operation modes.

All of the operation modes, which can take the symmetry of ϕ_2 and ϕ_3, are generated according to (16), because parameters p and q with (16) and (18) never generate the same combination of l, m, and n, and because they generate all of the possible combinations of l, m, and n. The two different modes, which are given by taking one of the doubled signs in (16) with the same p and q, have the same resonance frequency. These degenerate modes correspond to clockwise and counter clockwise rotational phase eigen-excitations.

The field variation along the ferrite post axis (z axis) never affects the mode classification since the modes are classified owing to the symmetry in the x–y plane. Therefore, mode numbers along the z axis, which can be obtained by superimposition

of traveling waves expressed as (1), are omitted in the mode representation.

The resonance frequency for each eigen-excitation is never different from that for a standing wave in the x–y plane, since only the linear superimposition of the standing wave is made to obtain the traveling waves. The resonance frequency was determined for the idealized boundary conditions at the end of the ferrite post [2]. The lowest operation mode is given by $l = 1$, $m = -1$, and $n = 0$.

The resonance frequency split for the rotational phase eigen-excitations is related to the circulator bandwidth and the circulation direction. Resonance frequency variation due to permeability variation is given as follows [5]:

$$\frac{\Delta\omega^{\pm}}{\omega} = -\frac{\int (H^{\pm *} \cdot \Delta\tilde{\mu} H^{\pm})\, d\tau}{2\int \mu_0 |H^{\pm}|^2\, d\tau} \tag{19}$$

where μ_0 is the permeability when the ferrite is demagnetized, $\Delta\tilde{\mu} = \tilde{\mu} - \mu_0$, $H^{\pm}$ denotes magnetic field for rotational phase eigen-excitations, and $d\tau$ denotes the volume integral element.

When anisotropy is weak, $\Delta\tilde{\mu}$ may be approximated as follows:

$$\Delta\tilde{\mu} \fallingdotseq \begin{pmatrix} 0 & -j\kappa & 0 \\ j\kappa & 0 & 0 \\ 0 & 0 & 0 \end{pmatrix}. \tag{20}$$

Using (19) and (20),

$$\frac{\Delta\omega^{\pm}}{\omega} \fallingdotseq \frac{\kappa}{\mu} \frac{\int \mathrm{Im}(Hx^{\pm} Hy^{\pm *})\, d\tau}{\int |H^{\pm}|^2\, d\tau}$$

$$= \frac{\kappa}{\mu} \frac{\int \{\mathrm{Im}(Hx^{\pm})\mathrm{Re}(Hy^{\pm}) - \mathrm{Re}(Hx^{\pm})\mathrm{Im}(Hy^{\pm})\}\, d\tau}{\int |H^{\pm}|^2\, d\tau}. \tag{21}$$

When the ferrite post is completely short or open circuited at the two ends, the integrals along the ferrite axis in the numerator and the denominator are the same. Therefore, the volume integrations can be replaced by surface integration. In this case, the resonance frequency split is independent of the field variation along the ferrite post axis.

In the present approximation, the resonance frequency splits for the two rotational phase eigen-excitations are equal and opposite, as seen from (17) and (21).

For the lowest operation modes,

$$\frac{\Delta\omega^{\pm}}{\omega} = \pm \frac{\sqrt{3}}{2} \frac{\kappa}{\mu}. \tag{22}$$

The preceding result indicates a bandwidth of about two times compared with that of a cylindrical ferrite post lowest mode. Circulation directions are the same as those of the lowest cylindrical mode.

Acknowledgment

The author wishes to thank Y. Matsuo, A. Tomozawa, Y. Katoh, and Dr. H. Kaneko for their encouragement and guidance during the course of this work.

References

[1] B. Owen, "The identification of modal resonances in ferrite loaded waveguide Y-junctions and their adjustment for circulation," *Bell System Tech. J.*, vol. 51, pp. 595–627, Mar. 1972.
[2] Y. Akaiwa, "Operation modes of a waveguide Y circulator," *IEEE Trans. Microwave Theory Tech.* (Short Papers), vol. MTT-22, pp. 954–960, Nov. 1974.
[3] J. Helszajn and F. C. Tan, "Design data for radial-waveguide circulators using partial-height ferrite resonators," *IEEE Trans. Microwave Theory Tech.*, vol. MTT-23, pp. 288–298, Mar. 1975.
[4] N. Ogasawara and T. Noguchi, "Modal analysis of the dielectric slab of the normal triangular cross section," *Papers of the Technical Group of Microwave*, IECE Japan, June 1974 (in Japanese).
[5] R. F. Harrington, "*Time-Harmonic Electromagnetic Field*," New York: McGraw-Hill, 1961.

Electromagnetic Fields Induced Inside Arbitrary Cylinders of Biological Tissue

TE-KAO WU, MEMBER, IEEE, AND
LEONARD L. TSAI, MEMBER, IEEE

***Abstract*—The electromagnetic field induced inside arbitrary cross-sectioned cylinders of biological tissue is analyzed by integral equation and moment method techniques. A TM or TE plane wave incidence is assumed, and the cylinders consist of bone or muscle and may be multi-layered. The integral equations are of the *surface* type, and are derived via vector Green's theorem and boundary conditions. Surface and interior fields for both a one-layer and two-layer circular cylinder are found to have excellent agreements with the exact eigenfunction expansion results, thus validating the numerical method. Extensive results are presented for arbitrary cross-section cylinders, with among these an arm model composed of an elliptical outer muscle layer and a circular bone at the center. The field plots throughout the cylinder interior thus obtained should be useful in diagnostics of microwave hazards, particularly in predictions of the so-called "hot spots."**

I. Introduction

Biological effects of microwave radiation is an area of current concern [1]. The mechanisms by which electromagnetic fields penetrate biological tissues, and the potential hazards they pose, are just beginning to be investigated. Analytical predictions in the area have so far been rather limited. Primarily, treatments have been confined to structures which conform to a separable coordinate system (e.g., spheres or circular cylinders) [2]–[4]. For more realistic models with varied and arbitrary contours, the versatility of numerical techniques, i.e., moment method solution of integral equations, which have been extensively employed in other electromagnetic problems, should prove to be particularly advantageous.

In this short paper, coupled surface integral equations (SIE's) are first derived via Maxwell's equations, Green's theorem, and boundary conditions. The geometry of the analytical model to be treated consists of arbitrarily contoured cylinders (infinitely long in the z direction) of biological tissue illuminated by a TM or TE plane wave. The method is similar to that used by Tong [5], but differs significantly from the work of Livesay and Chen [6]. The solution of the integral equations for the surface fields then employs flat pulse expansion and point matching. Once the surface fields are found, fields everywhere interior to the cylinder are then readily determined.

To test the validity of this method, homogeneous circular cylinders of muscle and fatty tissue are first studied. The surface fields thus computed by integral equation methods are compared with the exact eigenfunction expansion results. Surface fields on homogeneous elliptical cylinders are next obtained to illustrate the arbitrary geometry capabilities of the integral equation solution. For a more complex structure, i.e., a two-layered composite cylinder of circular cross section, the surface fields obtained by the numerical solution are also compared with the exact solution. The extension in this next case is for an arm model

Manuscript received April 14, 1975; revised June 28, 1976.
The authors are with the Department of Electrical Engineering, University of Mississippi, University, MS 38677.